

# A Theoretical Study of Electron Mobility Reduction due to Acoustic Phonon Modulation in a Free-Standing Semiconductor Nanowire

Junichi Hattori<sup>\*†</sup>, Shigeyasu Uno<sup>\*†</sup>, Nobuya Mori<sup>†</sup>, and Kazuo Nakazato<sup>\*†</sup>

<sup>\*</sup>Department of Electrical Engineering and Computer Science, Graduate School of Engineering, Nagoya University  
Furo-cho, Chikusa-ku, Nagoya 464-8603, Japan

Phone: +81-52-789-2794, Fax: +81-52-789-3139, Email: j\_hattori@echo.nuee.nagoya-u.ac.jp, uno@nuee.nagoya-u.ac.jp

<sup>†</sup>Department of Electronic Engineering, Graduate School of Engineering, Osaka University  
2-1 Yamada-oka, Suita, Osaka 565-0871, Japan

<sup>‡</sup>SORST JST, Japan

**Abstract**—Impacts of modulated acoustic phonons on electron transport in a free-standing cylindrical semiconductor nanowire are theoretically studied. We formulate the electron scattering rate and mobility limited by the intra-valley acoustic phonon scattering mechanism, using bulk and modulated acoustic phonons in a [001]-directed Si nanowire. The scattering rate calculated using modulated acoustic phonons is larger than that with bulk phonons, and therefore the mobility is smaller when modulated acoustic phonons are incorporated. These results are attributed to an increase of the form factor due to acoustic phonon modulation. The form factor increase has a universality independent of wire material and radius.

**Index Terms**—acoustic phonon, electron-phonon interaction, gate-all-around, electron mobility

## I. INTRODUCTION

Recently, Si nanowire metal-oxide-semiconductor field-effect transistors (MOSFETs) have received considerable attention as one of the promising devices for future electronics due to their improved short channel immunity [1], [2]. In predicting device performance, precise modeling of electron mobility is needed. At room temperature, the intra-valley acoustic phonon scattering plays an important role as an electron mobility limiting mechanism. Acoustic phonons in wire structures are modulated due to the mechanical mismatch at interfaces between different materials, and therefore they differ from bulk phonons [3], [4], [5]. The impacts of such modulated acoustic phonons on electron transport, particularly the comparison with those of bulk phonons, are of great interest. Acoustic phonon modulation is known to have significant impacts on electron transport for plate structures [6], [7]. For wire structures, some authors reported that electron scattering rate calculated using modulated acoustic phonons is larger than that with bulk phonons for III-V semiconductors, low temperature and intra-lowest-subband scattering [8], [9], [10]. However, in-depth studies of the impacts of modulated acoustic phonons on electron transport (such as effects on electron mobility, comparison with the results obtained using bulk phonons, developing their model, and investigating their mechanism) are still lacking.

In this paper, we theoretically study interactions between electrons and modulated acoustic phonons in a free-standing cylindrical semiconductor nanowire. We formulate electron scattering rate and mobility limited by the intra-valley acoustic phonon scattering, where the differences between bulk and modulated acoustic phonons are encapsulated in the form factor. The form factors for modulated acoustic phonons are larger than those for bulk phonons regardless of electron states, wire material and radius. The form factor increase directly leads to increase in electron scattering rate and reduction in mobility, which is confirmed for a [001]-directed Si nanowire. In addition, when properly normalized, the form factor increase shows a universality for wire material and radius.

## II. MODULATED ACOUSTIC PHONONS

First of all, we review modulated acoustic phonons in a free-standing cylindrical semiconductor nanowire. For details, refer to the literatures [3], [11], [12]. In general, when a longitudinal phonon wave impinges on a free surface, it is reflected as a mixture of longitudinal and transverse phonon waves. The same holds true for a transverse phonon wave incident. This phenomenon is referred to as mode conversion [12]. Mode conversion couples longitudinal and transverse waves in the nanowire, which are independent of each other in a bulk medium. Assuming that the nanowire is an isotropic continuum, acoustic phonons are described by Navier's equation:

$$\rho \frac{\partial^2 \mathbf{S}(\mathbf{r}, t)}{\partial t^2} = (\lambda + 2\mu) \nabla(\nabla \cdot \mathbf{S}(\mathbf{r}, t)) - \mu \nabla \times (\nabla \times \mathbf{S}(\mathbf{r}, t)), \quad (1)$$

where  $\mathbf{S}(\mathbf{r}, t)$  is the phonon displacement vector,  $\rho$  is the mass density, and  $\mu$  and  $\lambda$  are Lamé's constants. This equation is solved in the structure shown in Fig. 1, giving the general solution as a superposition of normal modes

$$\mathbf{S}(\mathbf{r}, t) = \sum_{\mathbf{q}} C_{\mathbf{q}} e^{i(m_p \theta + q_z z - \omega_{\mathbf{q}} t)} \mathbf{u}_{\mathbf{q}}(r), \quad (2)$$

where  $C_{\mathbf{q}}$  is a constant for a normal mode,  $m_p$  is the phonon azimuthal quantum number related to rotational symmetry,

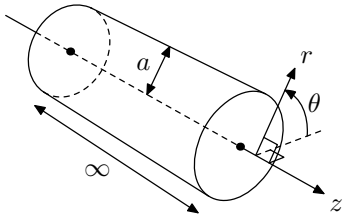


Fig. 1. Schematic view of a free-standing cylindrical semiconductor nanowire and the coordinates.

$q_z$  is the wave vector along the wire,  $\omega_{\mathbf{q}}$  is the frequency, and  $\mathbf{u}_{\mathbf{q}}(r)$  is the radial dependence of a normal mode. Three components of  $\mathbf{u}_{\mathbf{q}}(r)$  are as follows:

$$\begin{aligned} u_{\mathbf{q},r}(r) &= A_l q_l J'_{m_p}(q_l r) + i A_{t1} q_z q_t J'_{m_p}(q_t r) \\ &\quad + i A_{t2} m_p (q_t^2 + q_z^2) J_{m_p}(q_t r)/r, \\ u_{\mathbf{q},\theta}(r) &= i A_l m_p J_{m_p}(q_l r)/r - A_{t1} m_p q_z J_{m_p}(q_t r)/r \quad (3) \\ &\quad - A_{t2} (q_t^2 + q_z^2) q_t J'_{m_p}(q_t r), \\ u_{\mathbf{q},z}(r) &= i A_l q_z J_{m_p}(q_l r) + A_{t1} q_t^2 J_{m_p}(q_t r), \end{aligned}$$

where  $J_{m_p}(r)$  and  $J'_{m_p}(r)$  are Bessel functions of the first kind with order  $m_p$  and their first derivatives with respect  $r$ , respectively,  $A_l$ ,  $A_{t1}$  and  $A_{t2}$  are constants. The quantities  $q_l$  and  $q_t$  are the longitudinal and transverse phonon wave vectors in the radial direction and satisfy the following relation:

$$\rho \omega_{\mathbf{q}}^2 = (\lambda + 2\mu)(q_t^2 + q_z^2) = \mu(q_t^2 + q_z^2). \quad (4)$$

Applying free-surface boundary conditions, we obtain normal modes with discrete set of  $\omega_{\mathbf{q}}$  allowed for a given  $m_p$  and  $q_z$  as shown in Fig. 2. The calculation was done for Si, which has  $\rho = 2330 \text{ kg/m}^3$ ,  $\lambda = 93.4 \text{ GPa}$ ,  $\mu = 51.5 \text{ GPa}$ . The resulting normal modes are categorized into three submodes, torsional, dilatational and flexural modes. Torsional and dilatational modes are allowed for  $m_p = 0$ , while flexural modes for  $m_p = \pm 1, \pm 2, \pm 3, \dots$ . Among these submodes, dilatational and flexural modes contribute to electron scatterings through deformation potentials, whereas torsional modes do not because they do not cause local volume changes. Only longitudinal components of the phonon waves contribute to electron scatterings through acoustic deformation potential (ADP) scattering mechanism.

### III. ELECTRON-ACOUSTIC-PHONON INTERACTIONS

In formulating electron-acoustic-phonon interactions in the nanowire, we assume that the electron wave functions are written in the form

$$|mnk_z\rangle = \varphi_{mn}(r, \theta) e^{ik_z z} / \sqrt{L_z}, \quad (5)$$

where  $m$  and  $n$  are the quantum numbers of electron confinement in the azimuthal and radial direction, respectively,  $k_z$  is the electron wave vector along the wire, and  $L_z$  is the wire length. Solving Boltzmann transport equation in quasi-one-dimensional system using relaxation time approximation

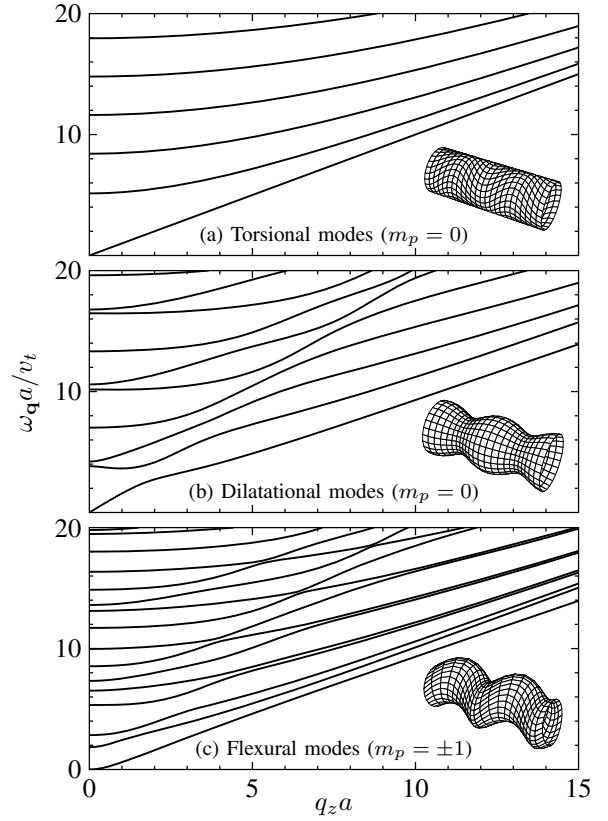


Fig. 2. Dispersion relations of acoustic phonons in a free-standing Si nanowire for (a) torsional, (b) dilatational, (c) lowest order flexural modes. Each horizontal axis represents phonon wave vector along the wire  $q_z$  multiplied by the wire radius  $a$ , and each vertical axis frequency  $\omega$  multiplied by  $a/v_t$ , where  $v_t = \sqrt{\mu/\rho}$  is the transverse sound velocity in bulk Si. The insets show the bird's-eye views of phonon waves at the wire surface.

and Fermi's golden rule gives the following electron back scattering rate for elastic ADP scattering:

$$\begin{aligned} \frac{1}{\tau_{mn}(k_z)} &= \sum_{m',n'} \frac{D_{ac}^2 k_B T_L}{2\hbar v_l^2 \rho} \int_{-\infty}^0 (I_{mn,m'n'}(q_z) \\ &\quad \times \delta((E_{m'n'} + E'_z) - (E_{mn} + E_z))(1 - (k'_z/k_z))) dk'_z, \quad (6) \end{aligned}$$

where  $(E_{mn}, E_{m'n'})$  are the electron energy levels of confinement in the nanowire before/after the scattering,  $(E_z, E'_z)$  are the electron energies along the wire,  $D_{ac}$  is the ADP constant,  $k_B$  is Boltzmann constant,  $T_L$  is the lattice temperature,  $v_l = \sqrt{(\lambda + 2\mu)/\rho}$  is the longitudinal sound velocity, and  $I_{mn,m'n'}(q_z)$  is the form factor, which represents overlap between the electron and phonon wave functions. For bulk phonons, the form factor is given by

$$I_{mn,m'n'}; \text{bulk} = \int_0^{2\pi} \int_0^a |\varphi_{m'n'}(r, \theta)|^2 |\varphi_{mn}(r, \theta)|^2 r dr d\theta, \quad (7)$$

which depends only on the initial/final electron states. On the other hand, for the modulated acoustic phonons, it is given by

$$\begin{aligned} I_{mn,m'n'}(q_z) &= (\rho L_z / v_l^2) \\ &\quad \times \sum_{m_p, q_l} \omega_{\mathbf{q}}^2 \left| \langle m'n' | A_l J_{m_p}(q_l r) e^{im_p \theta} | mn \rangle \right|^2, \quad (8) \end{aligned}$$

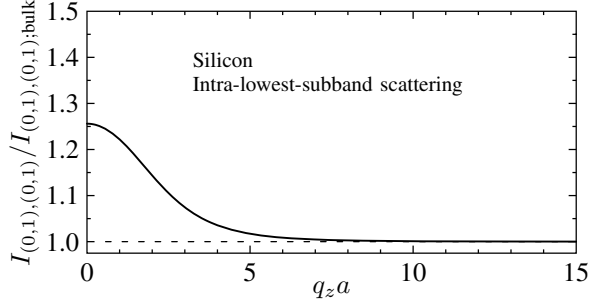


Fig. 3. Ratio of the form factor calculated using the modulated and bulk phonons, plotted as a function of phonon wave vector along the wire  $q_z$  multiplied by the wire radius  $a$ . The calculation was done for Si nanowire, for intra-lowest-subband scattering.

where the phonon wave vector along the wire  $q_z$  is equal to  $k'_z - k_z$  because of the momentum conservation, and the summation over  $q_l$  is taken for all discrete values allowed for a given  $q_z$  and  $m_p$ . Rewriting the electron scattering rate  $1/\tau_{mn}(k_z)$  as a function of  $E_z$ , we have

$$\frac{1}{\tau_{mn}(E_z)} = \frac{d_v D_{ac}^2 k_B T_L}{\rho \hbar^2 v_l^2} \sqrt{\frac{m_d^*}{2}} \times \sum_{m', n'} I_{mn, m' n'}(q_z) (E_z^{-1/2} + E_z'^{-1/2}) H(E_z'), \quad (9)$$

where  $E'_z = E_z + E_{mn} - E_{m' n'}$ ,  $d_v$  is the valley degeneracy,  $m_d^*$  is the electron density-of-state effective mass, and  $H(E)$  is Heaviside function. Using this scattering rate, ADP scattering limited electron mobility is written as

$$\mu_{mn} = (2ed_v \sqrt{2m_d^*} / \pi \hbar m_c^* N_{mn}) \times \int_0^\infty \frac{\partial F(E_{mn} + E_z)}{\partial E_z} \tau_{mn}(E_z) \sqrt{E_z} dE_z, \quad (10)$$

where  $m_c^*$  is the electron conductivity effective mass,  $N_{mn}$  is the electron density at the subband  $(m, n)$ , and  $F(E)$  is Fermi-Dirac distribution. Then, total mobility is given by

$$\mu_{ADP} = \frac{\sum_{m, n} N_{mn} \mu_{mn}}{\sum_{m, n} N_{mn}}. \quad (11)$$

In the above formulation, the differences between bulk and modulated acoustic phonons appear only in the form factor. Thus, the form factor is a key quantity in discussing the effects of the acoustic phonon modulation on electron transport.

Fig. 3 shows the form factor for intra-lowest-subband scattering ( $(m, n) = (m', n') = (0, 1)$ ) calculated using the modulated acoustic phonons, plotted as a function of phonon wave vector  $q_z$ . The vertical axis is divided by the form factor for bulk phonons, and the horizontal axis is multiplied by the wire radius  $a$ , so that the curve is valid for any wire radius. In the calculation, the electrons were confined to the nanowire due to infinite potential barrier, and the wire material was set to Si. Note that the form factor at small  $q_z a$  is larger than that for bulk phonons, while they are equal at large  $q_z a$ . Such a form factor increase has been confirmed for all initial/final electron states. The form factor increase leads to increase in the

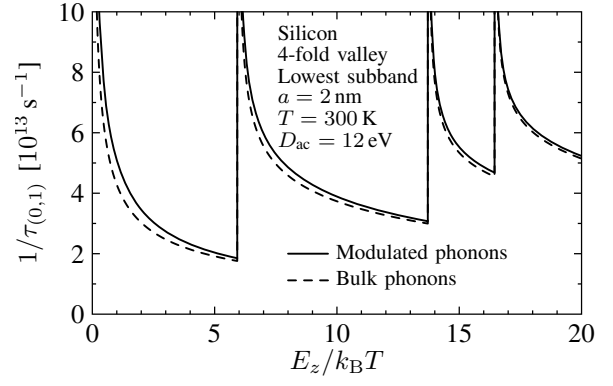


Fig. 4. ADP scattering rate of 4-fold valley electrons in the lowest subband in a [001]-directed free-standing Si nanowire with 2nm radius plotted as a function of electron energy along the wire  $E_z$  divided by the thermal energy.

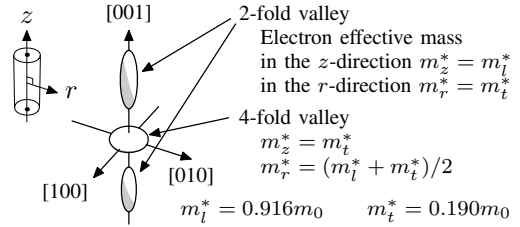


Fig. 5. Schematic view of the conduction band valleys in a [001]-directed free-standing Si nanowire.

electron scattering rate through (6) or (9), and hence reduction of the electron mobility. Fig. 4 shows the electron scattering rate (9) as a function of electron energy along the wire  $E_z$ . The calculation was done for electrons in the lowest subband in a Si nanowire with radius 2 nm. The Si nanowire is assumed to be directed to the [001] direction, then conduction band valleys are of two types, 2-fold and 4-fold valley as illustrated in Fig. 5. The results shown in Fig. 4 correspond to the 4-fold valley. In addition,  $D_{ac}$  was set to 12 eV,  $T_e$  and  $T_L$  were both 300 K. Note that the scattering rate calculated using the modulated acoustic phonons is larger than that obtained for bulk phonons. Also note that the scattering rate diverges at  $E_z = E_{m' n'} - E_{mn}$ , because the electron density of states for the final state  $E_{m' n'}$  diverges. Fig. 6(a) shows the total electron mobility limited by the intra-valley acoustic phonon scattering (11) plotted as a function of wire radius  $a$ . In the calculation, the electron density was set to  $2.0 \times 10^9 \text{ m}^{-3}$ . As can be expected from the scattering rate increase, the reduction of electron mobility due to the acoustic phonon modulation is observed. The mobility reduction becomes more significant with decreasing radius as shown in Fig. 6(b). The dotted lines in Fig. 6(a) are the results of the following formula obtained using bulk phonons and an assumption that electrons exist only in the lowest subband:

$$\mu^{(0,1);bulk} = \frac{\pi e \hbar^2 v_l^2 \rho J_1^A(R_{0,1}) a^2}{d_v D_{ac}^2 k_B T_L m_c^* \sqrt{2m_d^*}} \int_0^\infty F(E_{(0,1)} + E_z) dE_z \times \left( \int_0^1 J_0^A(R_{0,1} r) r dr \int_0^\infty \frac{F(E_{(0,1)} + E_z)}{\sqrt{E_z}} dE_z \right)^{-1}, \quad (12)$$

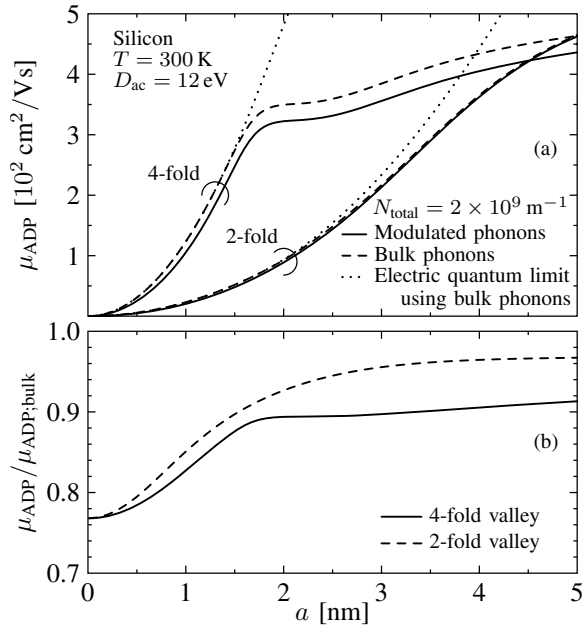


Fig. 6. (a) Intra-valley acoustic phonon scattering limited electron mobility for 2- and 4-fold valley electrons in a [001]-directed free-standing Si nanowire plotted as a function of wire radius  $a$ . (b) Ratio of mobility calculated using modulated acoustic phonons to that calculated using bulk phonons.

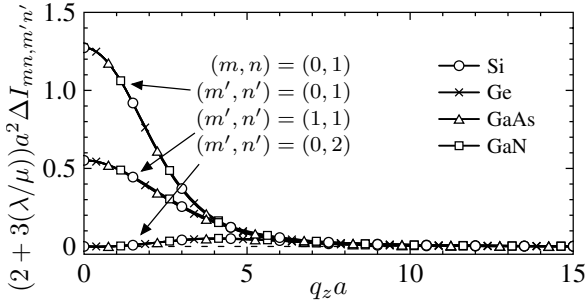


Fig. 7. Universal form factor increase for intra- and inter-subband scatterings plotted for various wire materials.

where  $R_{0,1}$  is the first positive zero of Bessel function of the first kind with order zero. This formula is in excellent agreement with the numerical results for bulk phonons at small radius. With increasing radius, however, electrons in the lowest subband are excited to higher subbands due to narrower energy gaps, and consequently, they undergo more frequent scattering. Therefore, at large radius, the electron mobility numerically calculated using bulk phonons deviates from (12).

#### IV. UNIVERSALITY IN ELECTRON-MODULATED-ACOUSTIC-PHONON INTERACTIONS

Fig. 7 shows the form factor increases  $\Delta I_{mn,m'n'} \equiv I_{mn,m'n'} - I_{mn,m'n';bulk}$  for intra- and inter-subband scatterings plotted for different wire materials, Si ( $\lambda/\mu \approx 1.82$ ), Ge (0.848), GaAs (0.895) and GaN(3.99). The vertical axis is multiplied by  $(2 + 3(\lambda/\mu))a^2$ . The form factor increase is observed for all the cases, moreover the curves do not depend on wire material. These characteristics of the form

factor increase have been confirmed for arbitrary initial/final electron states and wire material having positive  $\lambda/\mu$ . Fig. 7 indicates that  $\zeta \equiv 1/(2 + 3(\lambda/\mu))$  is a good parameter in comparing the impact of the acoustic phonon modulation on electron transport between different materials. Introducing the bulk modulus  $K$ ,  $\zeta$  is rewritten as  $\mu/3K$ . The Lamé's second constant  $\mu$  is the equivalent for the shear modulus, therefore a material which can be easily deformed by uniform pressure while not by shear stress has large  $\zeta$  and the modulated acoustic phonons significantly affect electron transport.

#### V. CONCLUSIONS

In conclusion, we have theoretically studied the interactions between electrons and modulated acoustic phonons in a free-standing cylindrical semiconductor nanowire. In formulating the interactions, the differences between bulk and modulated acoustic phonons have been encapsulated in the form factor. The form factor calculated using modulated acoustic phonons is larger than that with bulk phonons regardless of electron states, wire material and radius. This increase directly leads to increase in electron scattering rate and reduction in mobility, which has been confirmed for a [001]-directed Si nanowire. In addition, it has been found that the form factor increase has a universality independent of wire material and radius.

This research was partially supported by the Ministry of Education, Science, Sports and Culture, Grant-in-Aid for Young Scientists (B) No. 18760251 (2006) and No. 20760221 (2008), as well as the Global COE Program "Center for Electronic Devices Innovation". The authors would like to thank Tatematsu Foundation for financial support.

#### REFERENCES

- [1] K. H. Yeo *et al.*, "Gate-all-around (GAA) twin silicon nanowire MOSFET (TSNWFET) with 15 nm length gate and 4 nm radius nanowires," in *IEDM Tech. Dig.*, 2006, pp. 539–542.
- [2] N. Singh *et al.*, "Ultra-narrow silicon nanowire gate-all-around CMOS devices: impact of diameter, channel-orientation and low temperature on device performance," in *IEDM Tech. Dig.*, 2006, pp. 547–550.
- [3] V. G. Grigoryan and D. G. Sedrakyan, "Quantization of the phonon spectrum in wires (filaments)," *Sov. Phys. Acoust.*, vol. 29, pp. 281–283, 1983.
- [4] N. Nishiguchi, "Guided acoustic phonons in quantum wires: theory of phonon fiber," *Jpn. J. Appl. Phys.*, vol. 33, pp. 2852–2858, 1994.
- [5] M. A. Stroschio, Y. M. Sirenko, S. Yu, and K. W. Kim, "Acoustic phonon quantization in buried waveguides and resonators," *J. Phys.: Condens. Matter*, vol. 8, pp. 2143–2151, 1996.
- [6] L. Donetti, F. Gámiz, J. B. Roldán, and A. Godoy, "Acoustic phonon confinement in silicon nanolayers: effect on electron," *J. Appl. Phys.*, vol. 100, pp. 13701–13707, 2006.
- [7] S. Uno and N. Mori, "Analytical description of intravalley acoustic phonon limited electron mobility in ultrathin Si plate incorporating phonon modulation due to plate interfaces," *Jpn. J. Appl. Phys.*, vol. 46, pp. L923–L926, 2007.
- [8] S. Yu, K. W. Kim, M. A. Stroschio, G. J. Iafrate, and A. Ballato, "Electron-acoustic-phonon scattering rates in cylindrical quantum wires," *Phys. Rev. B*, vol. 51, pp. 4695–4698, 1995.
- [9] —, "Electron interaction with confined acoustic phonons in cylindrical quantum wires via deformation potential," *J. Appl. Phys.*, vol. 80, pp. 2815–2822, 1996.
- [10] N. Nishiguchi, "Electron scattering due to confined and extended acoustic phonons in a quantum wire," *Phys. Rev. B*, vol. 54, pp. 1494–1497, 1996.
- [11] B. A. Auld, *Acoustic Fields and Waves*. New York: Wiley, 1973.
- [12] K. F. Graff, *Wave Motion in Elastic Solids*. New York: Dover, 1991.